

Figure 1. Mass spectrum of the product obtained from the reaction between $\text{Mn}_2(^{12}\text{CO})_{10}$, $\text{Mn}_2(^{13}\text{CO})_{10}$, and ^{13}CO (76 min, 120 °C). The ^{13}CO used in these studies was 93.8% ^{13}C , 9.3% ^{17}O , and 1.5% ^{18}O ; accordingly, the $\text{Mn}_2(^{13}\text{CO})_{10}$ that was prepared from this ^{13}CO only approached ~94% ^{13}C content. The simulated spectrum^{1,5} for a CO dissociative based reaction using a half-life of 55 min (the range in half-life measurements, 45 ± 10 min, was due to minor temperature variations in the reaction conditions) is shown by dotted lines. Under identical reaction conditions but with an argon atmosphere, there was CO interchange between the manganese dimers. Roughly, 90% of the overall reaction under argon can be described as a pairwise exchange of CO. There was some buildup of mass 395, which can be interpreted as a result of some dissociation, 10%, of the dimer into mononuclear fragments. This could be either from fragmentation (or dimerization) of $\text{Mn}_2(\text{CO})_{10}$ or of $\text{Mn}_2(\text{CO})_9$. Note that the specific molecules $\text{Mn}_2(^{12}\text{C}^{16}\text{O})_{10}$, $\text{Mn}_2(^{13}\text{C}^{16}\text{O})_{10}$, and $\text{Mn}_2(^{12}\text{C}^{16}\text{O})_5(^{13}\text{C}^{16}\text{O})_5$ have the respective amu values of 390, 400, and 395.

exchange in $\text{Mn}_2(\text{CO})_{10}$ cannot proceed through a rate-determining Mn–Mn bond scission step and is fully consistent with the mechanism outlined in eq 1. Also, there was no major competing (nonproductive with respect to ligand exchange) reaction involving Mn–Mn bond scission at 120–150 °C.⁸ We suggest that the Mn–Mn bond energy in $\text{Mn}_2(\text{CO})_{10}$ substantially exceeds the 22 kcal/mol value most recently estimated⁴ (the enthalpy of activation for $\text{P}(\text{C}_6\text{H}_5)_3$ substitution in $\text{Mn}_2(\text{CO})_{10}$ is 37 kcal/mol^{6a}). Our results confirm the original Wawersik and Basolo^{6a} mechanistic proposal for $\text{Mn}_2(\text{CO})_{10}$ ligand-substitution reactions. This basic mechanistic scheme is also supported by the extensive studies of Atwood and co-workers^{6b} and those of Schmidt et al.^{6c}

Analogously, the reaction of $\text{Mn}_2(\text{CO})_{10}$ and $\text{Mn}_2(^{13}\text{CO})_{10}$ with *tert*-butyl isocyanide showed no evidence of Mn–Mn bond scission in the formation of $\text{Mn}_2(\text{CO})_9(\text{CNR})$ at 80 °C in benzene solution (Figure 2, supplementary material). Also, this reaction as catalyzed by Pd on charcoal proceeded at 25 °C without (1% or less) Mn–Mn bond scission, (Figure 3, supplementary material). Similar results were obtained with $\text{Re}_2(^{12}\text{CO})_{10}$ and $\text{Re}_2(^{13}\text{CO})_{10}$ isocyanide reactions. The half-life of the $\text{M}_2(\text{CO})_{10}$ uncatalyzed isocyanide reactions are about one-hundredth those for CO or $(\text{C}_6\text{H}_5)_3\text{P}$ reactions. Accordingly, the mechanism of the isocyanide reaction appears to be different from that for CO or for $(\text{C}_6\text{H}_5)_3\text{P}$ (eq 1); kinetic analyses of the Mn and Re isocyanide reactions are in progress.

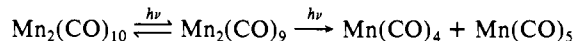
Reaction of $\text{Mn}_2(\text{CO})_{10}$ and $\text{Mn}_2(^{13}\text{CO})_{10}$ with $(\text{C}_6\text{H}_5)_3\text{P}$ in octane at 120 °C was analyzed in the early reaction stages (less than 1 half-life for the fastest⁹ reaction of the $\text{Mn}_2(\text{CO})_9\text{P}(\text{C}_6\text{H}_5)_3$ product with ^{13}CO). The mass spectrometric analysis of the residual $\text{Mn}_2(\text{CO})_{10}$ and the product $\text{Mn}_2(\text{CO})_9\text{P}(\text{C}_6\text{H}_5)_3$ showed

(8) At 150 °C, there appears to be scission of the Mn–Mn bond, but the percentage contribution of this process to the overall ligand-exchange reaction can be no more than 5%.

(9) Ligand exchange of $\text{Mn}_2(\text{CO})_9\text{P}(\text{C}_6\text{H}_5)_3$ with phosphines and phosphites was found to be very rapid as was originally reported by Wawersik and Basolo.^{6a}

no evidence (1% level) of Mn–Mn bond scission (Figure 4, supplementary material). Analysis of the bis-phosphine product was precluded by the short reaction times and because neither an EI nor a CI mass spectrum could be obtained for this complex.

Irradiation (Pyrex filtered) of the CO reaction with $\text{Mn}_2(\text{CO})_{10}$ and $\text{Mn}_2(^{13}\text{CO})_{10}$ clearly established that Mn–Mn bond breaking is a significant process under these conditions although our data do not distinguish between a predominant $\text{Mn}_2(\text{CO})_{10} \rightarrow 2\text{Mn}(\text{CO})_5$ and a predominant or competing photolytic process¹⁰ of



Quantitative photolysis studies, using labeled Mn (and Re) carbonyls, are in progress to establish whether this reaction is precisely a one-photon process.

The technique employed to distinguish unambiguously between M–CO and M–M bond scission reactions in $\text{Mn}_2(\text{CO})_{10}$ ligand substitution reactions is applicable generally to polynuclear metal carbonyl complexes, and we are applying this procedure to cobalt, iron, and ruthenium carbonyl complexes.

Acknowledgment. This research was supported by the National Science Foundation. N.J.C. thanks the CSIR and the University of the Witwatersrand for financial support while on sabbatical leave. We especially thank Sherri Ogden and Leah Zebre of the UCB Mass Spectrometric Facility for assistance in the mass spectrometric analyses.

Registry No. $\text{Mn}_2(\text{CO})_{10}$, 10170-69-1; $\text{P}(\text{C}_6\text{H}_5)_3$, 603-35-0; $(\text{CH}_3)_3\text{CNC}$, 7188-38-7.

Supplementary Material Available: Experimental procedure and Figures 1–4 for observed mass spectrometric data in the ^{13}CO – $\text{Mn}_2(\text{CO})_{10}$ reaction, the $(\text{CH}_3)_3\text{CNC}$ reaction with $\text{Mn}_2(\text{CO})_{10}$ and $\text{Mn}(^{13}\text{CO})_{10}$, the $(\text{CH}_3)_3\text{CNC}$ reaction with $\text{Mn}_2(\text{CO})_{10}$ and $\text{Mn}(^{13}\text{CO})_{10}$, catalyzed by Pd on charcoal, and the $(\text{C}_6\text{H}_5)_3\text{P}$ reaction with $\text{Mn}_2(\text{CO})_{10}$ and $\text{Mn}_2(^{13}\text{CO})_{10}$ (7 pages). Ordering information is given on any current masthead page.

(10) See ref 1 and also see: Rothberg, L. J.; Cooper, N. J.; Peters, K. S.; Vaida, V. *J. Am. Chem. Soc.* **1982**, *104*, 3536.

Birhythmicity and Compound Oscillation in Coupled Chemical Oscillators: Chlorite–Bromate–Iodide System¹

Mohamed Alamgir and Irving R. Epstein*

Department of Chemistry
Brandeis University, Waltham, Massachusetts 02254

Received January 27, 1983

The recent success of systematic approaches to the design of chemical oscillators^{2–4} has been accompanied by increased interest in more complex dynamical phenomena such as chemical chaos.⁵ Just as the first deliberately designed chemical oscillator² was constructed by coupling two bistable systems, one may ask what phenomena might arise if two oscillatory reactions were linked through a common species.

Heilweil et al.⁶ and Cooke⁷ have investigated the Belousov–

(1) Part 17 in the series Systematic Design of Chemical Oscillators. Part 16: Alamgir, M.; Orbán, M.; Epstein, I. R., submitted for publication in *J. Phys. Chem.*

(2) De Kepper, P.; Epstein, I. R.; Kustin, K. *J. Am. Chem. Soc.* **1981**, *103*, 2133–2134.

(3) Orbán, M.; De Kepper, P.; Epstein, I. R. *J. Am. Chem. Soc.* **1982**, *104*, 2657–2658.

(4) Alamgir, M.; De Kepper, P.; Orbán, M.; Epstein, I. R. *J. Am. Chem. Soc.*, in press.

(5) Turner, J. S.; Roux, J.-C.; McCormick, W. D.; Swinney, H. L. *Phys. Lett.* **1981**, *85A*, 9–12.

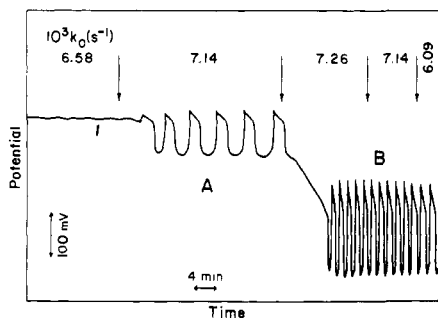


Figure 1. Birhythmicity in the chlorite–bromate–iodide system. Potential is that of Pt electrode vs. $\text{Hg}/\text{Hg}_2\text{SO}_4$ reference electrode. At times indicated by the arrows, flow rate is changed. Flow rate in each time segment (measured as reciprocal residence time k_0) is shown at top. Note that A state and B state are both stable at $k_0 = 7.14 \times 10^{-3} \text{ s}^{-1}$. Fixed constraints: $T = 25^\circ\text{C}$, $[\text{I}^-]_0 = 6.5 \times 10^{-4} \text{ M}$, $[\text{BrO}_3^-]_0 = 2.5 \times 10^{-3} \text{ M}$, $[\text{ClO}_2^-]_0 = 1.0 \times 10^{-4} \text{ M}$, $[\text{H}_2\text{SO}_4]_0 = 0.75 \text{ M}$.

Zhabotinsky (BZ) and Briggs–Rauscher systems, respectively, with two or more independently oscillatory organic substrates present. Both of these studies, which were done under batch (closed system) conditions, showed the surprising sequence of oscillations characteristic of one substrate followed by a quiescent period followed by a further series of oscillations characteristic of a second substrate. Maselko⁸ has studied the bifurcation behavior of a mixed substrate BZ system in a stirred-flow reactor (CSTR).

In perhaps the most thorough theoretical investigation of the phenomena that may arise from the coupling of chemical oscillators, Decroly and Goldbeter⁹ considered a flow system containing two allosteric enzymes for which the product of one constitutes the substrate of the other. In addition to regimes in which only a single stationary or oscillatory state is stable, they found smaller regions of phase space that exhibit hard excitation (stability of both a stationary and an oscillatory state), chaos (stable aperiodic oscillation), and birhythmicity (two different stable oscillatory states). While hard excitation^{10,11} and chaos^{5,12} have been observed thus far in several chemical systems, no experimental evidence has previously been reported for birhythmicity.

With the growing array of oscillatory systems now available,¹³ it has become possible to construct an inorganic system resembling in certain respects the coupled enzyme reaction studied by Decroly and Goldbeter.⁹ We report here on experiments involving chlorite, bromate, and iodide in a CSTR. Not only are both the ClO_2^- – I^- ¹¹ and the BrO_3^- – I^- reactions oscillatory, but iodide reacts with bromate to yield bromide, and ClO_2^- – BrO_3^- – Br^- is still a third oscillatory reaction.¹⁴ The chlorite–bromate–iodide system, in a narrow range of conditions, exhibits not only birhythmicity but also another new phenomenon, a compound oscillation in which one oscillator appears to be entrained by another so as to create a single oscillator with a complex waveform.

In Figure 1, we show the observed birhythmicity and hysteresis between the two modes of oscillation. At the same values of temperature, input concentrations, and flow rate, the system can exist in either a low-potential, high-amplitude oscillatory state (A) or a high-potential, low-amplitude oscillatory state (B). Transitions between the states can be induced not only by changes in the flow rate but also by sufficiently large one-time perturbations with oxidants (e.g., bromate, chlorite, permanganate) to generate

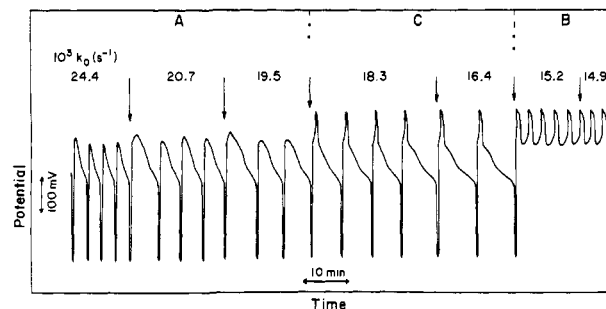


Figure 2. Compound oscillation (C) between A and B states as flow rate is changed. Fixed constraints as in Figure 1, except $[\text{I}^-]_0 = 4.0 \times 10^{-4} \text{ M}$.

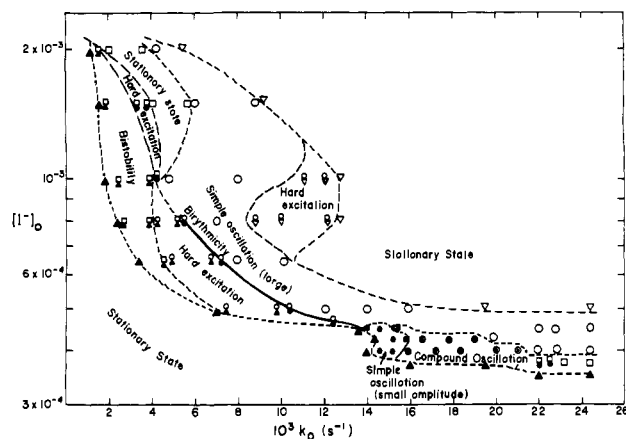


Figure 3. Phase diagram in the k_0 – $[\text{I}^-]_0$ plane (fixed constraints as in Figure 1): O, oscillatory state A; ●, oscillatory state B; ⊙, compound oscillation C; ⊞, birhythmicity, A and B both stable; ▲, high-potential stationary state; ▼, low-potential stationary state; □, intermediate-potential steady state. Combinations of two symbols imply bistability between the corresponding states.

the A \rightarrow B transition and reductants (e.g., iodide, sulfite) for the reverse transition.

The compound oscillation is illustrated in Figure 2. At high flow rate, we have the A state, and at low flow rate the B state. In an intermediate range these states merge into a single complex oscillation. Note that at the upper end of the compound oscillation range the frequency is very close to that of the pure A oscillator and that the frequency increases as k_0 decreases, like the A state but unlike the B state. It thus appears that the B oscillator is entrained by the lower frequency, higher amplitude A oscillator.

In Figure 3, we show a section of the phase diagram in the flow rate–iodide plane. In addition to the two simple and one compound oscillating states, there exist three different stable stationary states. In agreement with the calculation of Decroly and Goldbeter,⁹ the regions of birhythmicity and complex oscillation are found to be relatively small.

On comparison of the present results with those obtained for the component subsystems,^{4,11,14} it is tempting to identify the oscillatory states A and B with those of ClO_2^- – I^- and BrO_3^- – I^- , respectively. This identification is based upon similarities in waveform, amplitude, period, and absolute potential. A true understanding of the full system, however, must await the development of mechanisms for the component oscillators and a more thorough experimental study.

Whether the observations reported here will be of use in understanding the proposed role⁹ of coupled oscillators and birhythmicity in biochemical regulation remains to be seen. Our results do support the notion that the variety of chemical oscillators is now sufficient that almost any phenomenon predicted from the study of nonlinear differential equations may be realized in an appropriately designed chemical system.

Acknowledgment. We thank Jerzy Maselko, György Bazsa, Robert Olsen, and Kenneth Kustin for helpful discussions. This

(6) Heilweil, E. J.; Henchman, M. J.; Epstein, I. R. *J. Am. Chem. Soc.* **1979**, *101*, 3698–3700.

(7) Cooke, D. O. *Int. J. Chem. Kinet.* **1982**, *14*, 1047–1051.

(8) Maselko, J., submitted for publication.

(9) Decroly, O.; Goldbeter, A. *Proc. Natl. Acad. Sci. U.S.A.* **1982**, *79*, 6917–6921.

(10) De Kepper, P. C. *R. Seances Acad. Sci., Ser. C* **1976**, *283C*, 25–28.

(11) Dateo, C. E.; Orbán, M.; De Kepper, P.; Epstein, I. R. *J. Am. Chem. Soc.* **1982**, *104*, 504–509.

(12) Orbán, M.; Epstein, I. R. *J. Phys. Chem.* **1982**, *86*, 3907–3910.

(13) For a review, see: Epstein, I. R.; Kustin, K.; De Kepper, P.; Orbán, M. *Sci. Am.* **1983**, *248* (3), 112–123.

(14) Orbán, M.; Epstein, I. R. *J. Phys. Chem.*, in press.

work was supported by Grant CHE8204085 from the National Science Foundation.

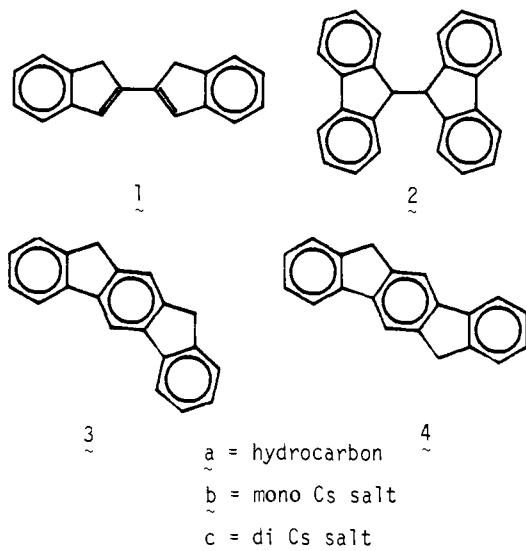
First and Second Acidity Constants for Some Indenyl and Fluorenyl Hydrocarbons: Coulombic Effects in Ion Triplets¹

Andrew Streitwieser, Jr.,* and Jon T. Swanson

Department of Chemistry, University of California
Berkeley, California 94720

Received November 22, 1982

We recently reported that the first and second ion pair pK' 's in the cesium cyclohexylamide (CsCHA)-cyclohexylamine (CHA) system for 9,10-dihydroanthracene differ by only 3.8 pK units.² We now report that for 2,2'-biindenyl (**1a**) and 9,9'-bifluorenyl



(**2a**) the formation of the dicesium salts of the dicarbanions (**1c** and **2c**) is hardly more difficult than formation of the cesium salts of the monocarbanions (**1b** and **2b**). For comparison, the ΔpK ($pK^2 - pK^1$) values are larger for 10,12-dihydroindeno[2,1-*b*]-fluorene (**3a**) and 6,12-dihydroindeno[1,2-*b*]-fluorene (**4a**). These results are rationalized by simple Coulombic considerations of ion triplet structures.

The pK measurement technique³ is based on a competitive equilibrium between a carbon acid (RH) and an indicator (InH) with their respective cesium salts; these salts exist primarily as contact ion pairs in CHA. The extension of the method to determination of second dissociation constants when the spectra of the mono- and dianion salts differ substantially (**3** and **4**) was summarized earlier.² Where the spectra overlap seriously, we use eq 1 and a least-squares technique. The derived first and second pK_{CsCHA} values are summarized in Table I.

$$A_{\lambda T} = \sum a_i A_{Ni} \quad A_{Ni} = \epsilon_i C_i \quad (1)$$

The values of the first pK' 's are unexceptional. The pK^1_{CsCHA} of **1** (19.81) is almost identical with that of indene ($pK_{CsCHA} = 19.93$). The pK^1_{CsCHA} of **2** (20.51) is substantially lower than that of fluorene ($pK_{CsCHA} = 23.04$) probably because of relief of steric strain in forming the carbanion; note that pK_{CsCHA} of 9-benzylfluorene is 1.77 pK units lower than that of fluorene.⁴ The first

Table I. Absorbance (nm) and pK_{CsCHA} Values

RH	λ_{max} ($10^{-3}\epsilon$)		pK^1_{CsCHA}	pK^2_{CsCHA}
	R^-Cs^+	$R^{2-}Cs_2^+$		
1	345 (26.1)	372 (32.0)	19.81 ^a	20.27 ^a
		391 (29.9)		
2	408 (6.2)	413 (16.0)	20.51 ^b	20.65 ^b
	3	331 (41.0)		
4	416 (20.0)	391 (36.0)	22.24 ^a	27.30 ^a
	472 (2.2)	413 (95.0)		
	500 (2.8)	467 (7.5)		
	533 (1.8)	499 (5.0)		
	370 (12.0)	355 (82.0)		
	392 (22.0)	428 (16.0)		
	482 (0.8)			
524 (1.0)				
	562 (0.8)			

^a ± 0.2 . ^b ± 0.3 .

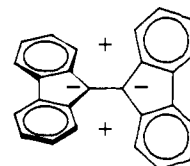


Figure 1. Ion triplet structure of dialkali cation salts of 9,9'-bifluorenyl (**2**).

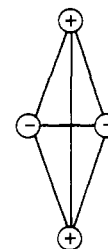


Figure 2. Coulomb interactions for a point charge model of a dication salt of a dicarbanion.

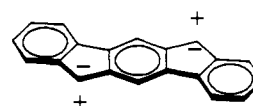


Figure 3. Ion triplet structure assumed for **4c**.

pK' 's of the indenofluorenes are slightly lower than for fluorene, as one might expect for phenyl-substituted fluorenes.

The pK^2_{CsCHA} values, however, are most unusual; ΔpK is 0.5 for **1** and only 0.14 for **2**. The pK' 's for **3** and **4** are greater, 3.4 and 5.1, respectively, and differ substantially from each other despite their similarity in structure.

The X-ray crystal structure of a dilithium salt of **2** has been reported;⁵ in this structure the two fluorenyl ring planes are twisted with respect to each other, and solvated Li^+ groups are placed above and below the central C-C bond (Figure 1). A similar structure is plausible for the dicesium salt and for the dicesium salt of **1**. In these structures the centers of negative charge in the cyclopentadienyl moieties are close together and give rise to significant electron repulsion. Nevertheless, a simple Coulomb treatment shows that it is this very proximity of charges in an ion triplet that provides added stabilization.

Consider the collection of point charges shown in Figure 2. For such a system the following equation holds for the electrostatic energy, E_{el} :

$$E_{el} = 1/R_{-} + 1/R_{++} - 4/R_{+-} \quad (2)$$

where R_{+-} is the distance between positive and negative charges. It is readily shown that E_{el} is negative in the R_{-}/R_{++} range 0.145-6.92; that is, for chemically significant structures the attraction of each negative charge equally to the two positive charges

(5) Walczak, M.; Stucky, G. D. *J. Organomet. Chem.* **1975**, *97*, 313.

(1) Carbon Acidity. 64. For paper 63 see: Streitwieser, A., Jr.; Juaristi, E. *J. Org. Chem.* **1982**, *47*, 768.

(2) Streitwieser, A., Jr.; Berke, C. M.; Robbers, K. *J. Am. Chem. Soc.* **1978**, *100*, 8271.

(3) Streitwieser, A., Jr.; Juaristi, E.; Nebenzahl, L. L. "Comprehensive Carbanion Chemistry"; Buncl, E., Durst, T., Eds.; Elsevier: New York, 1980; Chapter 7.

(4) Streitwieser, A., Jr.; Chang, C. J.; Reuben, D. M. E. *J. Am. Chem. Soc.* **1972**, *94*, 5730.